Sensing and Bio-Sensing Research 29 (2020) 100371

Contents lists available at ScienceDirect

Sensing and Bio-Sensing Research

journal homepage: www.elsevier.com/locate/sbsr

Deep learning in a sensor array system based on the distribution of volatile compounds from meat cuts using GC–MS analysis

Shoffi Izza Sabilla[a,b,*], Riyanarto Sarno[a,b], Kuwat Triyana[c,d,*], Kenshi Hayashi[e]

[a] Department of Informatics, Faculty of Intelligent Electrical and Informatics Technology, Institut Teknologi Sepuluh Nopember (ITS) Sukolilo, Surabaya 60111, Indonesia
[b] ITS Halal Center, Institute of Research and Community Service, Institut Teknologi Sepuluh Nopember, Surabaya 60111, Indonesia
[c] Department of Physics, Faculty of Mathematics and Natural Sciences, Gadjah Mada University, Sekip Utara BLS 21, Yogyakarta 55281, Indonesia
[d] Institute of Halal Industry and Systems (IHIS) Universitas Gadjah Mada, Sekip Utara Yogyakarta, 55281, Indonesia
[e] Department of Electronics, Faculty of Information Science and Electrical Engineering, Kyushu University, 744 Motooka, Fukuoka 819-0395, Japan

ARTICLE INFO

Keywords:
Deep learning
Chromatography
Electronic nose
Meat cuts
GC–MS

ABSTRACT

Generally, people distinguish the type of meat by looking at the color, texture, and even aroma of meat. These three methods have less effective approaches to distinguish the types of meat from meat cuts. Some researchers analyze the differences in the aroma of meats by using laboratory equipment, which is gas chromatography–mass spectrometry (GC–MS). This tool is mostly accurate, but it requires some time to determine the meat types completely. Moreover, the analysis process using GC–MS is also complicated. Nowadays, the electronic nose (e-nose) is a promising technology because it has a faster process of identifying various food types with reasonable production costs. Hence, the development of an e-nose for distinguishing volatile compounds from some meat types is appealing. Not only to determine the type of meat, but this study can also differentiate the part of the body from the meat, which has never been done by previous researchers. GC–MS was used as ground truth for the e-nose system, which helped the results to meet the standards. To achieve the objective in differentiating two meat cuts from three types of meat, this study uses statistical parameters for extraction feature, PCA for reducing the dimension, and deep learning.

Furthermore, to get more improvements from the previous researches, this study aims to optimize the parameters of deep learning. The result of the proposed method was compared to several machine learning algorithms that were used in previous studies, i.e., k-nearest neighbor ($k-$NN), support vector machine (SVM), Multi-Layer Perceptron (MLP), and basic deep learning. The experimental results showed that e-nose could detect meat cuts for 120 s, and the proposed method provides a significant improvement.

1. Introduction

Meat is one of the most often foods to consume as a source of protein [1]. There are many types of meat for consumption, from the most common animals such as livestock and poultry to the animals that are only eaten in certain areas such as camels, horses, and other wild animals. Beef, pork, and chicken are some types of meat that mostly consume by people. Generally, people distinguish the type of meat by looking at the color, texture, and even aroma of meat. However, these three methods have less effective approaches to distinguish meat cuts. There are several ways to find the differences between meat cuts from beef, pork, chicken in chemical analysis, by using GC–MS, FT-IR spectroscopy [2], PCR [3], NIR, ELISA, and LC-MS. In the Kayley research team [4], there are differences between the results of the volatile compound in the body parts of the cow that are grilled using GC–MS, such as ribeye, loin strips, and top sirloin. In addition, other research also shows the differences between volatile compounds in raw and cooked beef cuts using HS-SPME-GC–MS [5]. Beef cuts used in this research are rib, flank, and shank. Gas chromatography (GC) is mainly used to quantitatively analyze the amounts of compounds and mass spectrometry (MS) to analyze the molecular structure of the analyte compounds. This equipment is mostly accurate, but it takes time to finish detecting the meat cuts. Furthermore, the analysis process using GC–MS is also complicated because it must be operated by experts.

Nowadays, the electronic nose (e-nose) is a promising technology due to the faster process of identifying various food types with reasonable production costs. In recent years, the e-nose has been developed as a multifunctional instrument for detecting food quality [6–9],

* Corresponding authors at: Department of Physics, Faculty of Mathematics and Natural Sciences, Gadjah Mada University, Sekip Utara BLS 21, Yogyakarta 55281, Indonesia.
E-mail addresses: shoffi12@mhs.if.its.ac.id (S.I. Sabilla), triyana@ugm.ac.id (K. Triyana).

https://doi.org/10.1016/j.sbsr.2020.100371
Received 1 May 2020; Received in revised form 18 July 2020; Accepted 21 July 2020

Table 1
Recent Publications using *E*-nose with Meat Samples.

Years	Samples	GC–MS	Methods	Ref
2019	Duck adulteration in mutton	SPME	PLS, LDA, FLDA	[23]
2019	Minced beef and pork	HS-SPME	PLS, LDA	[24]
2019	Beef, chicken, pork	–	PCA, SVM	[25]
2019	Freshness of pork, beef, mutton	–	PCA, DFA	[26]
2019	Beef quality monitoring	–	QDA, SVM, ANN, ANFIS, k-NN	[27]

Acronyms used: Partial least square, PLS; linear discriminant analysis, LDA; Fisher linear discriminant analysis, FLDA; principal component analysis, PCA; support vector machine, SVM; discriminant factor analysis, DFA; quadratic discriminant analysis, QDA; artificial neural network, ANN; adaptive neuro-fuzzy inference system, ANFIS; k-nearest neighbor, k-NN.

environmental odor [10,11], and medical conditions [12,13]. *E*-noses can be used to analyze meat products, for example, pork adulteration in beef [14–16], classifying raw and cooked chicken [17], and sausage fermentation [15,18]. Previous researches that investigated the use of an e-nose on meat samples utilized an e-nose to differentiate the types of meat [19–22] and achieved positive results. However, the use of e-nose in that research was done without a standard validation from the GC–MS, considering this validation can be used as a strong ground-truth to develop e-nose. Table 1 shows some recent researches that using meat as a sample in e-nose testing. Two recent studies have been reported employing GC–MS along with an e-nose to detect duck adulteration in mutton [23] and minced beef and pork [24]. To the best of our knowledge, neither of the authors attempted to utilize the e-nose to differentiate meat cuts for three types of meat, which are beef, pork, and chicken. These meats have been validated using GC–MS, as can be seen in Table 1.

This research aimed to provide the electronic nose system (GeNose) with 8 MOS sensors to differentiate three types of meat (i.e., chicken, pork, beef) and expected to perform faster and higher accuracy levels compared to the previous research. Not only to determine the type of meat, but this research can also differentiate the part of the body of meat, especially upper (body) and lower (leg) parts of the body, which has never been done by previous researchers, as shown in Table 1. Based on the chemical analysis of GC–MS, upper and lower parts of the body have differences. GC–MS was used to help as the references and strong ground-truth to the difference of volatile compounds from GeNose. Besides, the electronic nose system used machine learning to differentiate between two meat cuts from three types of meat. Thus, there are six classes to be built. Previous research has been successfully classified three types of meats, and the accuracy was 96.2% using PCA as a dimension reduction and SVM as a machine learning [25]. This process will be complicated, as the goals to differentiate two parts of the body from each meat type because it has very similar signal results. This is a requirement to increase accuracy by using more classes. Deep learning is known as a good approach to solve complex problems [26,27], and many types of research employ this method nowadays. Of the recent e-nose researches listed in Table 1, none of them have implemented the proposed deep-learning method of this research. There are several types of deep learning, i.e., convolutional neural network (CNN) for image classification, deep belief network (DBN) for speech recognition, deep neural network (DNN) for signals, and recurrent neural network (RNN) for language translation.

This paper is organized into the following sections: Section 2 explains the proposed system, the details of the proposed method used in this research. Section 3 describes the results and evaluation of the experiment. The final section contains the conclusion of this paper.

Table 2
Gas sensors in the sensor array.

Sensor	Volatile compound target
TGS 813	Carbon monoxide (CO), methane, propane, isobutane, hydrogen, ethanol
TGS 822	Ethanol, acetone, methane, CO, isobutane, n-hexane, benzene
TGS 826	Ammonia, ethanol, isobutane, hydrogen
TGS 832	Chlorodifluoromethane (R22), dichlorodifluoromethane (R12), 1,1,1,2-tetrafluoroethane (R134a), ethanol
TGS 2600	CO, isobutane, ethanol, hydrogen, methane
TGS 2603	Ethanol, hydrogen, methyl mercaptan, trimethyl amine, hydrogen sulphide
TGS 2612	Methane, propane, isobutane, ethanol
TGS 2620	Ethanol, hydrogen, isobutane, CO, methane
SHT-15	Temperature, humidity

2. Proposed materials and method

2.1. Materials

2.1.1. Electronic nose system development

The proposed electronic nose system (GeNose) consisted of 8 MOS sensors, Taguchi series (TGS). It was also equipped with temperature and humidity sensors from the SHT-15 series. Based on the datasheet of each sensor, an 8-sensor array would be able to recognize the gases as described in Table 2 [28]. Previous research has calculated the cost of using a combination of sensors to build GeNose [25]. By using eight sensors, cost production can be reduced. Meat sample sensing with eight sensors produced different sensor response patterns [25]. Triyana [29,30] mentions that, generally, e-noses consist of numbers of component, i.e., a headspace system, a sample chamber, a sensor array chamber, a voltage divider circuit, a fan,

A data acquisition system, a power supply, a control circuit, an analog to digital converter (ADC), and an output terminal. The microcontroller used in this research is the Arduino system. Each data recording cycle of the dynamic headspace system consists of three processes: flushing, sensing, and purging. In the sensing process, the controller circuit turns the fan on for one minute, absorbs the volatile gases, and flows them into the sensor array chamber. The samples place in the controlled container (beaker glass), produce volatile gases, and the sensor system is reacted by increasing the sensitivity [31]. The temperature and humidity used in this study only to monitor the sensor chamber and does not perform in signal processing. The implementation of the proposed electronic nose system can be seen in Fig. 1.

2.1.2. Meat sample

The samples used in this study were three types of most frequent to consume, namely beef, chicken, and pork. The meat samples were bought on the market at the same time every day, 7 a.m., to ensure that

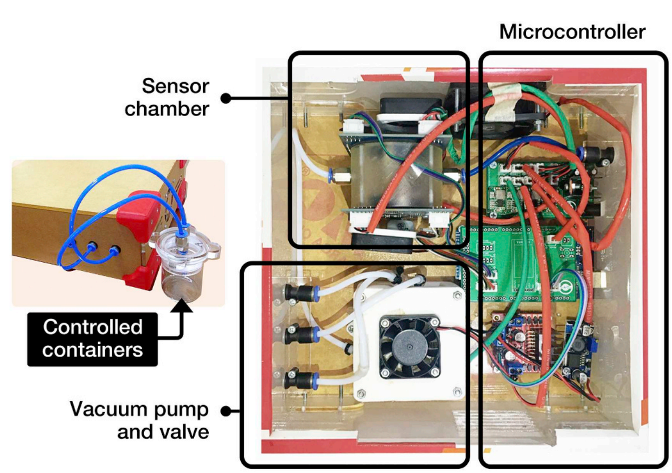

Fig. 1. The schematic of the electronic nose (GeNose) proposed in this study.

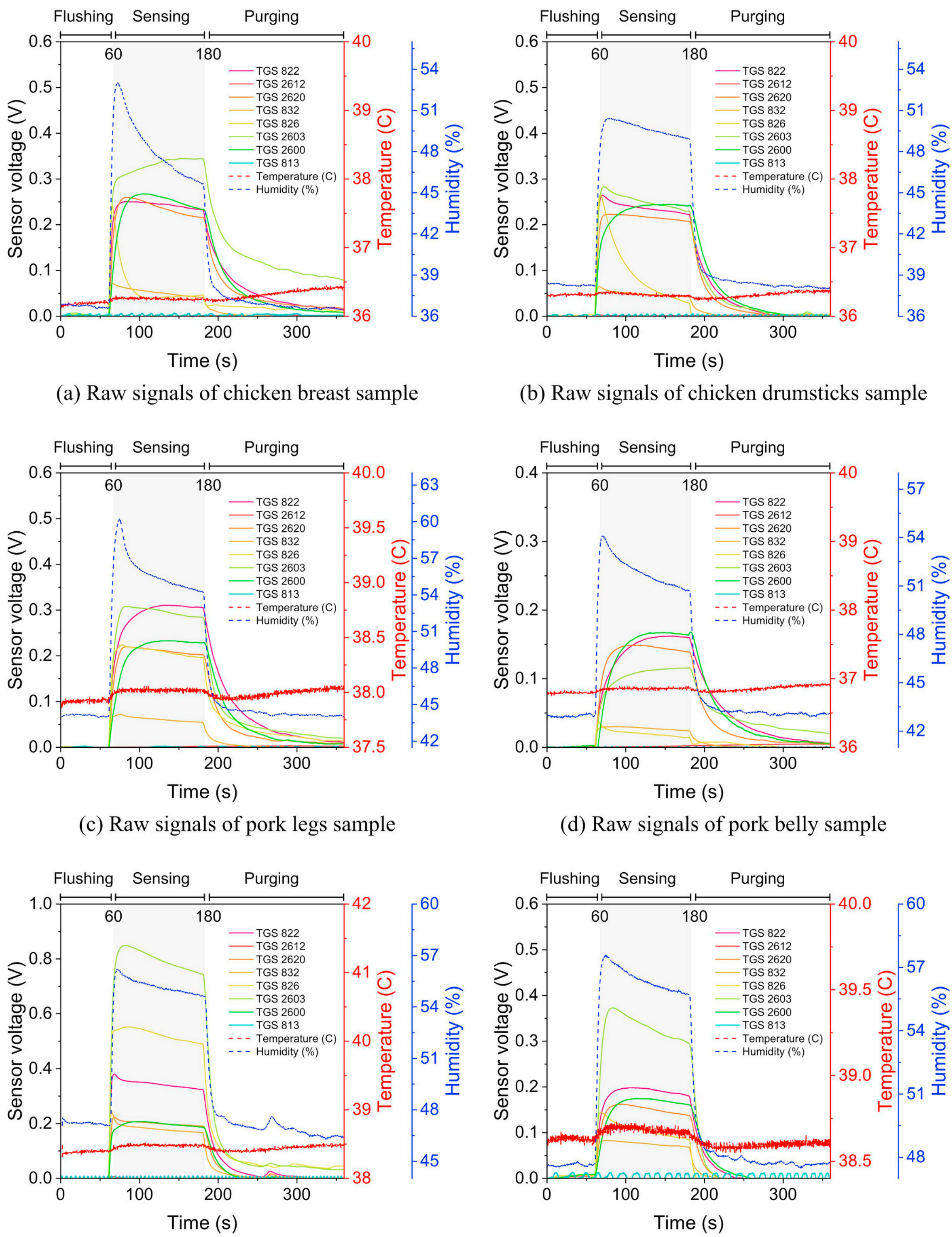

(a) Raw signals of chicken breast sample (b) Raw signals of chicken drumsticks sample

(c) Raw signals of pork legs sample (d) Raw signals of pork belly sample

(e) Raw signals of beef shank sample (f) Raw signals of beef ribs sample

Fig. 2. Signal responses from the ten sensors of the e-nose system.

the meat samples are fresh and not contaminated with bacteria. Two parts were selected for each type of meat, namely body, and leg. The samples collected were divided into six classes: 2 categories of beef, namely beef shank (BS) and beef ribs (BR); 2 categories of pork, namely pork legs (PL) and pork belly (PB); and two categories of chicken, namely chicken breast (CB) and chicken drumsticks (CD). The weight of each sample was identical (10 g). The meat samples were cut into small pieces and then put in a controlled container.

2.2. Method

2.2.1. Data acquisition

A sample test was carried out with the dynamic headspace system, 60 s of flushing, 120 s of sensing, and 180 s of purging or cleaning. Overall, one sample requires 360 s or 6 min for the whole process, and the data are stored every 100 milliseconds. A comparison of the six classes is shown in Fig. 2. The result comprised of 226 data in total divided into 45 chicken breast, 40 chicken drumsticks, 33 pork legs, 47 pork belly, 25 beef ribs, and 36 beef shank. As can be seen in Fig. 2, there is a slight difference in the signal results between the parts from the body and the leg of beef, chicken, and pork. This study only uses the data from the sensing stage, as the aroma produced from the sample in this stage is entering into the sensor chamber.

2.2.2. Proposed deep learning architecture

The output from GeNose was used in the signal processing to get the characteristics data using statistic method and utilized the machine learning as data processing. However, one of the problems that occurred using machine learning is the curse of dimensionality problem, where it is suffering to handle the amount of data input with a very high dimension. Principle component analysis (PCA) was used in this research to reduce the dimension from the data signal without losing any important information. Based on the eight gas sensors, eight raw data are obtained, and the extraction feature is done by using a statistical parameter with mean and standard deviation. As a result, the features are extracted into 16, which are eight mean and eight standard deviation. This feature is entered into the PCA process to reduce its dimension. Several component variations were given for the PCA, from 1, 2, 5, 6, 7, 10, 15, 20, 25. Therefore, the output of 16 features with n-dimension has been reduced. In total, n-dimension were generated to be used as x_n in the DNN for the input layer. Moreover, DNN was selected as the deep-learning method in this research because of its ability to calculate data signals [32–34]. This algorithm is part of an ANN (artificial neural network) algorithm that is appropriate for decision making. The most common understanding of a DNN is an artificial neural network that has more than one hidden neural layer [35]. According to the theory, this type of algorithm is capable of solving several cases that cannot be solved by an ANN algorithm [34]. It is an alternative to replace the ANN algorithm, which uses a large number of neurons in its hidden layer. DNN uses feed-forward and back-propagation, consisting of neurons that have weight as a connector. One layer of a neuron consists of one input layer, one or more hidden layers, and one output layer. The input layer receives the signal from outside, passes it to the first hidden layer and then to the output layer. Each neuron receives input and performs a dot operation with a weight (w), which sums the weight and adds a bias (b).

In the use of deep learning, several hyperparameters are generally used to get the best model, for example, the number of layers, number of neurons, activation functions, and dropouts. Hyperparameters are tuned by identifying the settings to get the best performance on the validation set. One way to determine the combination of Hyperparameters is to use Grid Search. Grid Search works by combining the values entered in Hyperparameters. The number of hidden layers used is based on the previous study [36]. This study has tried to add more hidden layers, but the results are far from the expectation. This research used several variations of the number of neurons for each hidden layer. The variations are 10, 20, 50, 100, 1000, and 10000. Based on the results of observation produced, 100 neurons are best for hidden layer 1, and 1000 neurons are best for hidden layer 2.

This paper proposes the architecture for the deep-learning system in Fig. 3 based on the optimal combination of hyperparameters. The first step is to calculate the weight (w), and bias (b) of the input and goes through the hidden layers, as shown in Eqs. (1) and (2). w_{injm} and b_{injm} are the weight and bias between the input layer and hidden layer 1, respectively. Input i and n describe n^{th} input, where j and m describe a line toward the neurons in hidden layer 1. The architecture has 1 input layer, 2 hidden layers, and 1 output layer. The output layer in this research was six classes of meat cuts. There is x_n inputs, i.e. i_1 to i_{16} and j_1 to j_{100}, respectively.

$$w_{i_nj_m} = \begin{bmatrix} w_{i_1j_1} & w_{i_1j_2} & w_{i_1j_3} & w_{i_1j_4} & \cdots & w_{i_1j_{97}} & w_{i_1j_{98}} & w_{i_1j_{99}} & w_{i_1j_{100}} \\ w_{i_2j_1} & w_{i_2j_2} & w_{i_2j_3} & w_{i_2j_4} & \cdots & w_{i_2j_{97}} & w_{i_2j_{98}} & w_{i_2j_{99}} & w_{i_2j_{100}} \\ \vdots & \vdots & \vdots & \vdots & \vdots & \vdots & \vdots & \vdots & \vdots \\ w_{i_{15}j_1} & w_{i_{15}j_2} & w_{i_{15}j_3} & w_{i_{15}j_4} & \cdots & w_{i_{15}j_{97}} & w_{i_{15}j_{98}} & w_{i_{15}j_{99}} & w_{i_{15}j_{100}} \\ w_{i_{16}j_1} & w_{i_{16}j_2} & w_{i_{16}j_3} & w_{i_{16}j_4} & \cdots & w_{i_{16}j_{97}} & w_{i_{16}j_{98}} & w_{i_{16}j_{99}} & w_{i_{16}j_{100}} \end{bmatrix} \tag{1}$$

$$b_{i_nj_m} = [b_{i_1j_1} \;\; b_{i_1j_2} \;\; b_{i_1j_3} \;\; \cdots \;\; b_{i_1j_{98}} \;\; b_{i_1j_{99}} \;\; b_{i_1j_{100}}] \tag{2}$$

After w and b have been obtained, the forward pass from input to hidden layer 1 is calculated. The formula for a forward pass expressed in Eq. (3). The activation function is used to activate or deactivate neurons in the layer. This function will transform input into a specific input. There are several types of activation functions, namely sigmoid, tanh, softmax, ReLu. Sigmoid function has been popular because it has a steady-state at 0 [37]. But Ian [37], on his book, mentioned that ReLU is currently more popular because it provides better results in many different settings. This study uses ReLU as an activation function. The input layer moves toward hidden layer 1 using the formula of ReLU activation $f(x) = \max(0, x)$, as shown in Eq. (4).

$$FF\_layer_1 = sum\left(\begin{bmatrix} (x_1) \\ (x_2) \\ \vdots \\ (x_{15}) \\ (x_{16}) \end{bmatrix} \times [w_{j_mk_h}]\right) + [b_{i_nj_m}] \tag{3}$$

$$Out_{layer_1} = ReLU(FF\_layer_1) = [\max(0, FF\_layer_1)] \tag{4}$$

The next step is calculating w and b from hidden layer 1 to hidden layer 2. ReLU is performed with 100 neurons in the second layer; therefore the bias is $b_{jk_{1000}}$. The six biases from hidden layer 2 are moved to the output layer. Softmax activation (σ) is used for the calculation from hidden layer 2 to the output layer, as shown in Eq. (5).

$$\sigma(a_w) = \frac{exp(a_w)}{\sum_{q=1}^{p}(a_w)} \tag{5}$$

The dropout value of hidden layer 2 was 0.1, and 1000 neurons were used. Hidden layer 1 and hidden layer 2 used ReLU activation. The architecture of the proposed DNN in this study used 500 epochs. The use of complex hyperparameters can lead to overfitting. Early stopping is used in deep learning to avoid overfitting when training a learner with an iterative method. Changes will be monitored for each iteration, and early stopping will work if there are no significant changes.

3. Results and discussion

3.1. The experiments of proposed method

Before the proposed method was designed, this research compared several classification methods along with their best parameters, i.e., multi-layer perceptron (MLP), K-nearest neighbor (KNN), and SVM. The MLP algorithm delivered the best accuracy of 84.95% by using the best ReLU activation parameters, with a total of 500 neurons in the hidden layer and nine components of PCA. The KNN algorithm delivered the best accuracy of 86.81% with the total neighbors of 4, by using the model weight of distance and nine components of PCA. The SVM algorithm delivered the best accuracy of 90.36%, by using parameter C of 10 and gamma(γ) of 0.1. However, according to the authors, the results were still not optimal due to the classification error rate, which was still above ± 10%.

This research was initiated some experimental models using DNN as can be seen in Table 3. The highest accuracy result of basic DNN with

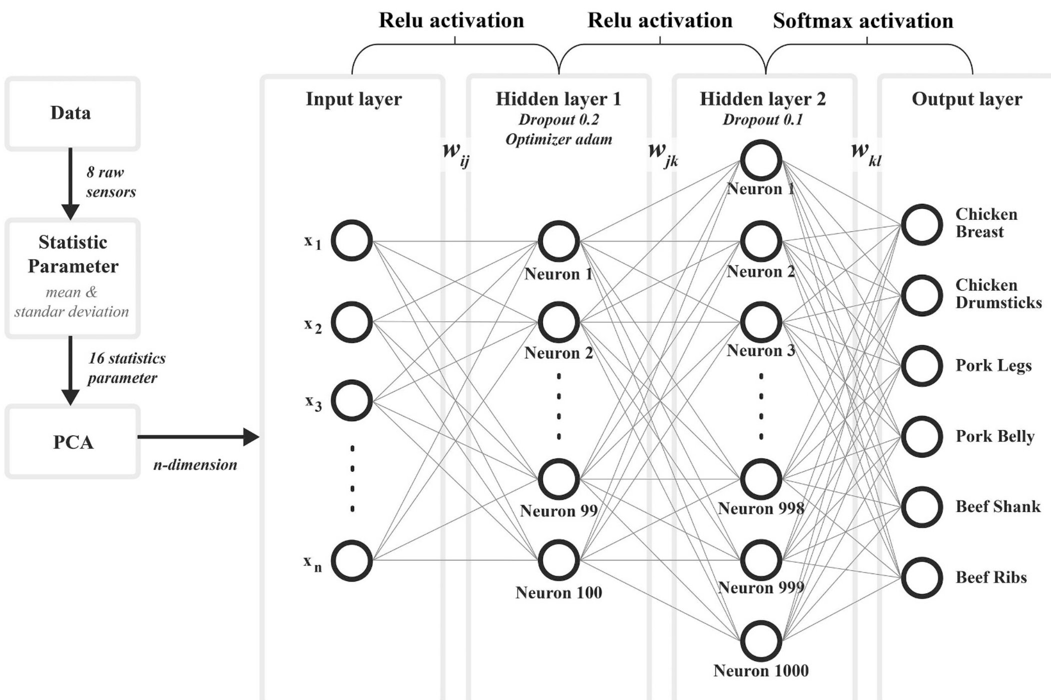

Fig. 3. Overview of the proposed deep-learning system.

Table 3
Results of Accuracy DNN with Optimized Parameter.

Model experiment	Optimized parameter details			Accuracy (%)
	Activation	Optimizer	Dropout	
Raw Data → DNN	Sigmoid	Adagrad	0.1	85.84%
			0.2	85.40%
		Adam	0.1	92.48%
			0.2	95.13%
	ReLU	Adagrad	0.1	96.02%
			0.2	95.13%
Raw Data → PCA → DNN	Sigmoid	Adagrad	0.1	88.05%
			0.2	86.73%
		Adam	0.1	94.25%
			0.2	95.13%
	ReLU	Adagrad	0.1	96.02%
			0.2	95.13%
Raw Data → Proposed method	ReLU	Adam	0.1	96.02%
Raw Data → PCA → Proposed method	ReLU	Adam	0.1	96.90%

unoptimized parameters was 96.02%. This accuracy was very significant with six classes, compared to the previous research, which was 96.2% for only three classes [25]. In the last experiment of DNN with optimized parameters, the accuracy was able to achieve a satisfying result of 98.88% using three classes. This result was increased by 2.68% from the previous research [25]. By using six classes to the proposed method with optimal parameters, the accuracy result was 96.90%, which showed significant results.

3.2. Evaluation for proposed method

Evaluation of the results of the proposed method was done using the confusion matrix method. The data are divided into two classes, namely the predicted class from the classifier result and the actual class from the initially known class data. In measuring performance using a confusion matrix, there are four states to represent the results of the classification process, namely true positive (TP), true negative (TN), false positive (FP), and false-negative (FN). Based on the number of TNs, FPs, FNs, and TPs, the values of precision, recall, and accuracy can be obtained. Precision describes the number of outcomes categorized as positive that are classified correctly, divided by the total data to be classified as positive. This value can be obtained from Eq. (6). Meanwhile, recall shows the percentage of positive outcomes that are classified correctly by the system. In binary classification, recall is known as sensitivity. Moreover, accuracy describes how accurately the system can classify data. The accuracy value is a comparison between correctly classified data and all data. The accuracy value can be obtained by Eq. (7).

$$Precision\ (P) = \frac{TP}{(TP + FP)} \times 100\% \tag{6}$$

$$Accuracy\ (Acc) = \frac{(TP + TN)}{(TP + TN + FP + FN)} \times 100\% \tag{7}$$

$$Sensitivity = TPR = \frac{TP}{P} = \frac{TP}{(TP + FP)} = 1 - FNR \tag{8}$$

$$Specificity = FPR = \frac{FP}{(FP + TN)} = 1 - TNR \tag{9}$$

Fig. 4 shows all generated confusion matrix for six classes, CB, CD, PL, PB, BS, which were classified correctly. Only one class showed incorrect predictions, namely the BR class. Five data were predicted incorrectly, i.e., they were categorized as CB instead of BR, one data was predicted as PB, and one data was predicted as BS. The evaluation results in Table 4 show that the value of TPR can be used to see the sensitivity, as shown in Eq. 12. When TPR and FPR are close to 1, the result is very sensitive and specific. The TPR and TNR results of the proposed method had a very sensitive value of 0.9690 and a specific value of 0.9938.

The receiver operating characteristic (ROC) curve is a technique to visualize, organize, and select classifications based on the performance of a classification algorithm. Each object is mapped into one element of the set of pairs, positive or negative. In the ROC curve, TPR is plotted on the y-axis, and FPR is plotted on the x-axis, as can be seen in Fig. 5. Classification results are bad if the ROC curve is close to the baseline or

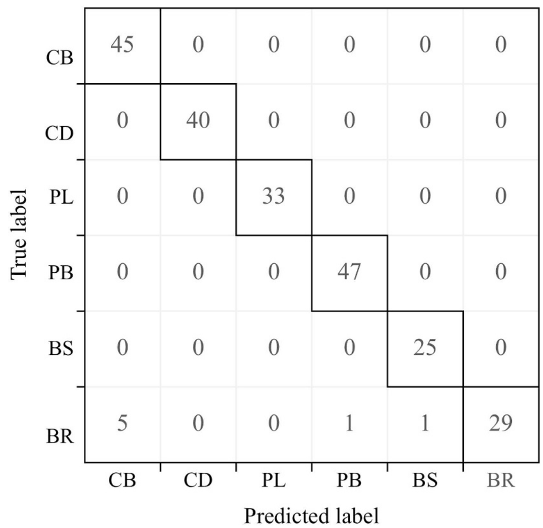

Fig. 4. Confusion matrix from DNN classification with optimized parameters.

in a transverse line (0.0). Classification results are good if the curve is close to point 1.0.

3.3. Measurement gas chromatography and mass spectrometry system

In order to get a better understanding of the chemical nature of the sensory differences between the three types of meat and the two categories of meat cuts, the volatile compounds were analyzed using GC–MS. The GC–MS system utilized laboratory equipment and glass tubes that are commonly used in analytical laboratories, for example, iceboxes, 1000-ml micropipettes, an analytical balance, stainless steel scissors, closed plastic containers, a Thermo GC–MS system with RT*x*5-MS capillary columns, Restech 30 m × 0.25 mm ID, 0.25 µm, polymethyl siloxane. The temperature of the injector was 240 °C with a water rate of 1.15. The samples were tested using the following procedure:

a) Slice twenty-five grams of meat sample into small pieces and put into a beaker glass;
b) Put the samples into a dry oven and set the temperature to 50 °C, wait for 6 h until the fat or oil tissue melts;
c) Once the melted solid oil separates, put it into a separating funnel for further purification by adding n-hexane reagents;
d) Mix the filtered, purified oil from the filter paper with sodium sulfate (Na_2SO_4) to bind the remaining water.

The concentration of volatile compounds in the meat samples was obtained by looking at the result of the peak area of the samples. This study showed a large contribution of volatile compounds in the percentage of TIC (%TIC). The sum percentage for each category was more than 50%. In total, 15 volatile components were identified in the raw material, matched the threshold, as can be seen in Table 5. These volatile compounds were generally the result of oxidation of fatty acid components of lipids. As can be seen in Table 5, two volatile compounds appeared consistently in all categories, i.e., tetradecane and tetradecane,2,6,10-trimethyl-. The tetradecane compounds had the highest concentrations, but different in each category. The highest concentration of tetradecane compounds was presented in the chicken meat from the leg and drumsticks, i.e., 39.31% of TIC, whereas the lowest percentage for tetradecane compounds was found in pork belly, i.e., 5.27%. In addition, there were several compounds in other categories that were presented. These can be a differentiator for the categories compared to one another. According to the result of GC–MS, parts from the body consistently had a higher TIC than parts from the legs.

3.4. Results of sample testing using GeNose provide with GC–MS

Among 8 MOS sensors from meat cuts of chicken, pig, and beef, GeNose was able to provide four sensors based on GC–MS results, which parts from the body consistently showed a higher TIC than parts from the legs. Sensor TGS 822, TGS 2620, TGS 832, TGS 813 also consistently showed a higher the signal response value than parts from the legs, which can distinguished parts from the body, as shown Fig. 6. By using these four sensors, the accuracy is 0.92035 or 92.04%, which is comparable to the results of GC–MS and performs very well to differentiate meat cuts. Therefore, this result validates the proposed e-nose system with GC–MS results.

4. Conclusions

In this research, GeNose was able to qualitatively differentiate and detected six classes with stage sampling for 120 s. This can also classified meat cuts into two categories for three types of meat, i.e., beef, pork, and chicken, with good results. The basic DNN produced satisfactory results, with an accuracy of 96.02% to differentiate six classes. The proposed optimal parameters for DNN could increase the accuracy by 0.88%, with the final accuracy result of 96.90%. This result also confirmed with the verification of quantitative analysis using GC–MS. GeNose reduced the sensors into 4 MOS sensors, which were sufficient to differentiate two categories for three types of meat, and the results were similar compared to GC–MS. The analysis from GC–MS also confirmed the sensitivity and selectivity of the electronic nose with appropriate results in detecting the difference between meats cuts.

GeNose is a rapid, accurate, low-cost, and environmentally friendly tool for differentiating meat cuts as a qualitative analysis. In future work, the percentage of volatile compounds in the sample will be predicted by using an electronic nose.

Table 4
Comparison of The Evaluation Results between Several Machine Learning and The Proposed Method.

Class	SVM			KNN			MLP			Proposed method		
	P	Recall	f-1 Score	*P*	Recall	f-1 Score	*P*	Recall	f-1 Score	*P*	Recall	f-1 Score
CB	0.91	0.89	0.90	0.89	0.87	0.88	0.89	0.87	0.88	0.90	1.00	0.95
CD	0.86	0.93	0.89	0.80	0.90	0.85	0.84	0.90	0.87	1.00	1.00	1.00
PL	0.92	1.00	0.96	0.83	0.91	0.87	0.85	0.85	0.85	1.00	1.00	1.00
PB	0.96	0.96	0.96	0.93	0.89	0.91	0.91	0.91	0.91	0.98	1.00	0.99
BS	0.83	0.80	0.82	0.87	0.80	0.83	0.82	0.72	0.77	0.96	1.00	0.98
BR	0.91	0.81	0.85	0.88	0.81	0.84	0.81	0.83	0.82	1.00	0.81	0.89
Acc	90.36%			86.81%			84.95%			96.90%		

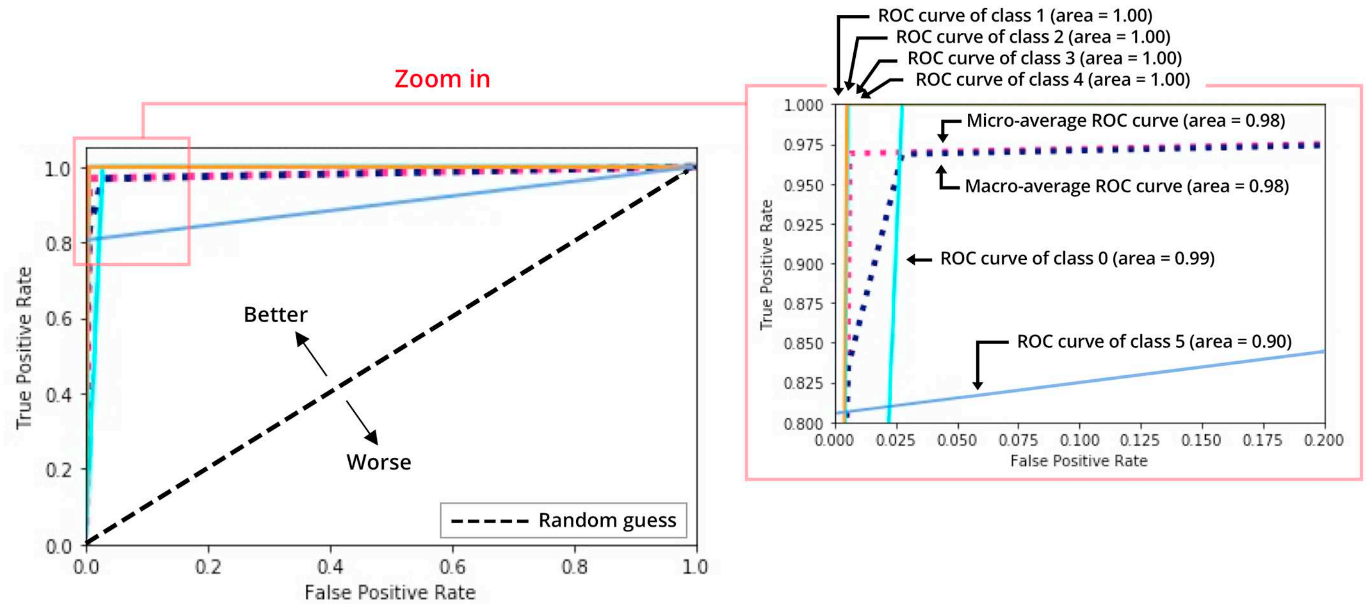

Fig. 5. ROC curve of detecting six classes of sample.

Table 5
Results of Screening Meat Cuts Using GC–MS.

Volatile compounds	CB	CD	PB	PL	BR	BS
9-hexadecenoic acid, hexadecyl ester, (*Z*)-	0	0	0.22	0	0	0.52
9-octadecenoic acid (Z)-, hexyl ester	0	0	0.24	0.52	0	0.69
Hexadecenoic acid, 1-(hydroxymethyl)-1,2-ethanediyl ester	2.10	0	0	0	0	0.59
9-octadecenoic acid (Z)-, hexyl ester	2.06	0	0	2.56	0	0.75
Hexadecane, 1,1-bis(dodecyloxy)-	0	0	0	2.56	0	0
Tetradecane	39.31	35.29	5.27	12.89	21.04	11.78
Tetradecane, 2,6,10-trimethyl-	12.49	9.79	1.91	5.05	6.51	3.86
Acetic acid, 3,7,11,15-tetramethyl-hexadecyl ester	0	0	0	0	7.27	6.52
cis-13-eicosenoic acid	0	0	0.23	1.35	1.64	0
Acetic acid, 3,7,11,15-tetramethyl-hexadecyl ester	0	0	0	0	7.27	0
1-hexadecanol, 2-methyl-	0	0	0.85	2.33	0	0
E,E,Z-1,3,12-nonadecatriene-5,14-diol	1.92	0	0.23	0	0	0.57

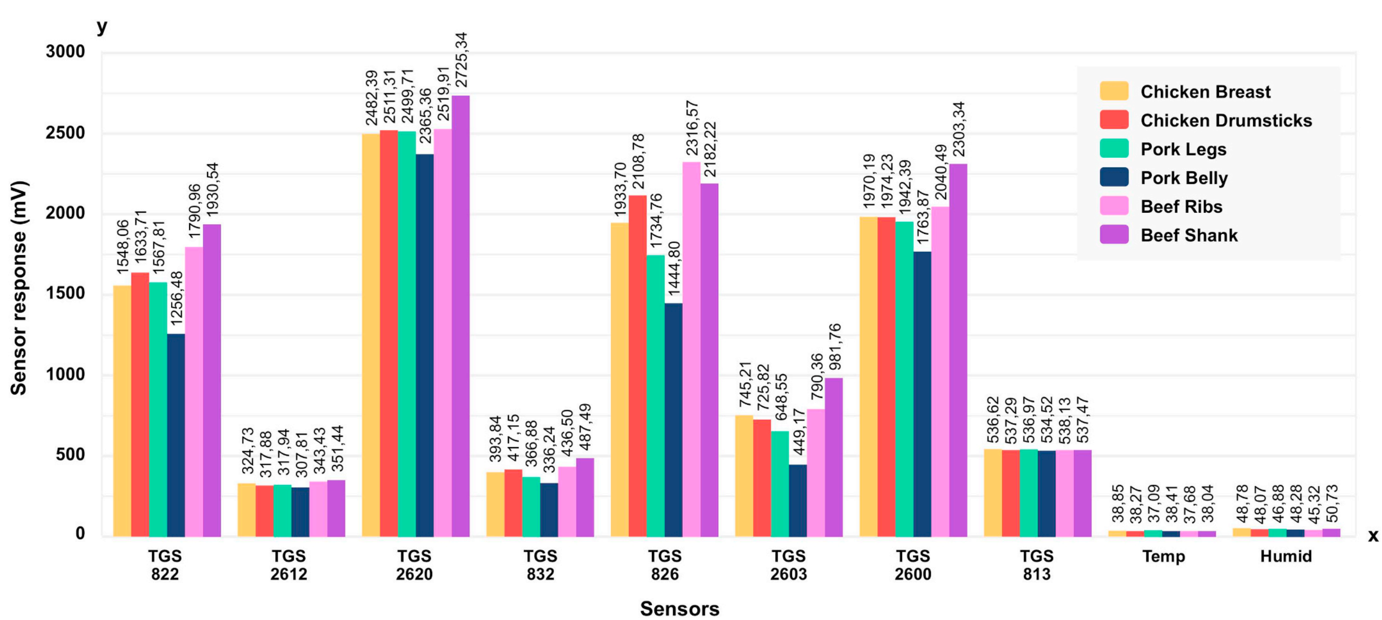

Fig. 6. Sensitivity differences for each sensor in detecting meat cut samples.

Declaration of Competing Interest

We declare that there are no conflicts of interest.

Acknowledgments

This research was funded by the Indonesian Ministry of Education and Culture, and the Indonesian Ministry of Research and Technology/ National Agency for Research and Innovation, under PMDSU Program managed by Institut Teknologi Sepuluh Nopember (ITS), and under World Class University (WCU) Program managed by Institut Teknologi Bandung (ITB), and under PTUPT Program managed by Universitas Gadjah Mada (UGM) research grant (Contract No. 340 2914/ UN1.DITLIT/DIT-LIT/PT/2020).

References

[1] L. Malek, W.J. Umberger, E. Goddard, Committed vs. uncommitted meat eaters: understanding willingness to change protein consumption, Appetite 138 (Jul. 2019) 115–126.
[2] M. Lucarini, A. Durazzo, J. Sánchez del Pulgar, P. Gabrielli, G. Lombardi-Boccia, Determination of fatty acid content in meat and meat products: The FTIR-ATR approach, Food Chem. 267 (Nov. 2018) 223–230.
[3] M.A.M. Hossain, S.M.K. Uddin, S. Sultana, S.Q. Bonny, M.F. Khan, Z.Z. Chowdhury, M.R. Johan, M.E. Ali, Heptaplex polymerase chain reaction assay for the simultaneous detection of beef, buffalo, chicken, cat, dog, pork, and fish in raw and heat-treated food products, J. Agric. Food Chem. 67 (29) (Jul. 2019) 8268–8278.
[4] K.R. Wall, C.R. Kerth, R.K. Miller, C. Alvarado, Grilling temperature effects on tenderness, juiciness, flavor and volatile aroma compounds of aged ribeye, strip loin, and top sirloin steaks, Meat Sci. 150 (Apr. 2019) 141–148.
[5] X. Wang, L. Zhu, Y. Han, L. Xu, J. Jin, Y. Cai, H. Wang, Analysis of volatile compounds between raw and cooked beef by HS-SPME–GC–MS, J. Food Process. Preserv. 42 (2) (Feb. 2018) e13503.
[6] V.S. Kodogiannis, A. Alshejari, A fuzzy-wavelet neural network model for the detection of meat spoilage using an electronic nose, 2016 IEEE International Conference on Fuzzy Systems, 2016 FUZZ-IEEE, 2016, pp. 710–717.
[7] S. Yudthavorasit, K. Wongravee, N. Leepipatpiboon, Characteristic fingerprint based on gingerol derivative analysis for discrimination of ginger (Zingiber officinale) according to geographical origin using HPLC-DAD combined with chemometrics, Food Chem. 158 (Sep. 2014) 101–111.
[8] S. Qiu, L. Gao, J. Wang, Classification and regression of ELM, LVQ and SVM for E-nose data of strawberry juice, J. Food Eng. 144 (Jan. 2015) 77–85.
[9] S.I. Sabilla, R. Sarno, J. Siswantoro, Estimating gas concentration using artificial neural network for electronic nose, Procedia Comput. Sci. 124 (Jan. 2017) 181–188.
[10] D. Kang, D.H. Lee, Energy and environment efficiency of industry and its productivity effect, J. Clean. Prod. 135 (Nov. 2016) 184–193.
[11] H. Kim, B. Konnanath, P. Sattigeri, J. Wang, A. Mulchandani, N. Myung, M.A. Deshusses, A. Spanias, B. Bakkaloglu, Electronic-nose for detecting environmental pollutants: signal processing and analog front-end design, Analog Integr. Circ. Sig. Process 70 (1) (Jan. 2012) 15–32.
[12] T. Seesaard, C. Sriphrapradang, T. Kitiyakara, T. Kerdcharoen, Self-screening for diabetes by sniffing urine samples based on a hand-held electronic nose, BMEiCON 2016 - 9th Biomedical Engineering International Conference, 2017, pp. 1–4.
[13] R. Sarno, Hariyanto, D.R. Wijaya, Detection of diabetes from gas analysis of human breath using e-Nose, Proceedings of the 11th International Conference on Information and Communication Technology and System, vol. 2018-Janua, ICTS 2017, 2018, pp. 241–246.
[14] L. Yang, T. Wu, Y. Liu, J. Zou, Y. Huang, V.S. Babu, L. Lin, Rapid Identification of Pork Adulterated in the Beef and Mutton by Infrared Spectroscopy, J. Spectrosc. 2018 (Feb. 2018) 1–10.
[15] J. Ha, S. Kim, J. Lee, S. Lee, H. Lee, Y. Choi, H. Oh, Y. Yoon, Identification of pork adulteration in processed meat products using the developed mitochondrial DNA-based primers, Korean J. Food Sci. Anim. Resour. 37 (3) (2017) 464–468.
[16] B. Kuswandi, A.A. Gani, M. Ahmad, Immuno strip test for detection of pork adulteration in cooked meatballs, Food Biosci. 19 (Sep. 2017) 1–6.
[17] M. Wettasinghe, T. Vasanthan, F. Temelli, K. Swallow, Volatile flavour composition of cooked by-product blends of chicken, beef and pork: a quantitative GC–MS investigation, Food Res. Int. 34 (2–3) (Jan. 2001) 149–158.
[18] The detection of foodborne bacteria on beef: the application of the electronic nose, Springerplus, vol. 2, Dec. 2013.
[19] S. Balasubramanian, S. Panigrahi, C.M. Logue, M. Marchello, C. Doetkott, Spoilage identification of beef using an electronic nose system, Vet. Microbiol. Prev. Med. Publ. Vet. Microbiol. Prev. Med. 47 (5) (2004) 1625–1633.
[20] O.S. Papadopoulou, E.Z. Panagou, F.R. Mohareb, G.-J.E. Nychas, Sensory and microbiological quality assessment of beef fillets using a portable electronic nose in tandem with support vector machine analysis, Food Res. Int. 50 (1) (Jan. 2013) 241–249.
[21] D.R. Wijaya, R. Sarno, A.F. Daiva, Electronic nose for classifying beef and pork using Naïve Bayes, 2017 International Seminar on Sensors, Instrumentation, Measurement and Metrology (ISSIMM), 2017, pp. 104–108.
[22] M. Ghasemi-Varnamkhasti, S.S. Mohtasebi, M. Siadat, S. Balasubramanian, Meat quality assessment by electronic nose (Machine Olfaction Technology), Sensors 9 (8) (Jul-2009) 6058–6083.
[23] Q. Wang, L. Li, W. Ding, D. Zhang, J. Wang, K. Reed, B. Zhang, Adulterant identification in mutton by electronic nose and gas chromatography-mass spectrometer, Food Control 98 (Apr. 2019) 431–438.
[24] D.E. Pavlidis, A. Mallouchos, D. Ercolini, E.Z. Panagou, G.J.E. Nychas, A volatilomics approach for off-line discrimination of minced beef and pork meat and their admixture using HS-SPME GC/MS in tandem with multivariate data analysis, Meat Sci. 151 (May 2019) 43–53.
[25] S. Sabilla, R. Sarno, K. Triyana, Optimizing threshold using Pearson correlation for selecting features of electronic nose signals, Int. J. Intell. Eng. Syst. 12 (6) (2019) 81–90.
[26] J. Chen, J. Gu, R. Zhang, Y. Mao, S. Tian, Freshness evaluation of three kinds of meats based on the electronic nose, Sensors 19 (3) (Jan. 2019) 605.
[27] D.R. Wijaya, R. Sarno, E. Zulaika, Noise filtering framework for electronic nose signals: an application for beef quality monitoring, Comput. Electron. Agric. 157 (Feb. 2019) 305–321.
[28] Naoyoshi Taguchi, TGS semiconductor gas sensors, Figaro Engineering Inc, 2013.
[29] K. Triyana, M. Taukhid Subekti, P. Aji, S. Nur Hidayat, A. Rohman, Development of electronic nose with low-cost dynamic headspace for classifying vegetable oils and animal fats, Appl. Mech. Mater. 771 (Jul. 2015) 50–54.
[30] S.N. Hidayat, A. Rusman, T. Julian, K. Triyana, A.C.A. Veloso, A.M. Peres, Electronic nose coupled with linear and nonlinear supervised learning methods for rapid discriminating quality grades of superior java cocoa beans, Int. J. Intell. Eng. Syst. 12 (6) (2019).
[31] A. Anyfantis, S. Blionas, Proof of concept apparatus for the design of a simple, low cost, mobile e-nose for real-time victim localization (human presence) based on indoor air quality monitoring sensors, Sens. Bio-Sensing Res. 27 (Feb. 2020) 100312.
[32] B. Kim, J. Kim, H. Chae, D. Yoon, J.W. Choi, Deep neural network-based automatic modulation classification technique, 2016 International Conference on Information and Communication Technology Convergence, 2016 ICTC, 2016, pp. 579–582.
[33] Y. Wang, D. Wang, A deep neural network for time-domain signal reconstruction, ICASSP, IEEE International Conference on Acoustics, Speech and Signal Processing - Proceedings, vol. 2015-August, 2015, pp. 4390–4394.
[34] K. Li, C.H. Lee, A deep neural network approach to speech bandwidth expansion, ICASSP, IEEE International Conference on Acoustics, Speech and Signal Processing - Proceedings, vol. 2015-August, 2015, pp. 4395–4399.
[35] T.P. Oliveira, J.S. Barbar, A.S. Soares, Computer network traffic prediction: a comparison between traditional and deep learning neural networks, Int. J. Big Data Intell. 3 (1) (2016) 28.
[36] R. Sarno, S.I. Sabilla, D.R. Wijaya, Hariyanto, Electronic nose for detecting multilevel diabetes using optimized deep neural network, Eng. Lett. Int. Assoc. Eng. 28 (1) (2020) 31–42.
[37] I. Witten, E. Frank, M. Hall, P. Christopher, Data Mining - 4th Edition Practical Machine Learning Tools and Techniques, 4th Ed, Morgan Kaufmann, 2016.